

Sl. No.	<p style="text-align: center;"><b>IIT Ropar</b>  <b>List of Recent Publications with Abstract</b>  <b>Coverage: June, 2021</b></p>
1.	<p><a href="#"><u>A Multi-Criteria Decision Approach to Select Contract Manufacturer for Sustainable Development of Automotive Products: an Integrated Framework</u></a>  PK Singh, P Sarkar - Process Integration and Optimization for Sustainability, 2021</p> <p><b>Abstract:</b> The increasing pressure on manufacturing organizations to produce eco-friendly products has led these organizations to select sustainable contract manufacturers for outsourcing their products. This study aims to develop an approach for selecting a contract manufacturer (CM), having the capability of producing environmentally sustainable automotive products for original equipment manufacturers (OEMs). A framework is proposed to achieve this task. This framework is developed by integrating two multi-criteria decision-making techniques (MCDM), viz. Analytical Hierarchy Process (AHP) and ViseKriterijumska Optimizacija I Kompromisno Resenje (VIKOR). The selection of the CM for producing eco-friendly automotive products is based on certain criteria (i.e., different life cycle stages of products to be considered by CM) and sub-criteria (i.e., various ecodesign practices to be implemented by CM under each life cycle stage of products). A total of 22 sub-criteria are selected on the basis of literature and expert's opinion from auto industry and academia. The application of the proposed research has been demonstrated through a case study which includes 4 alternative contract manufacturing companies related to automotive products. AHP method has been utilized to assign the weightage to different criteria and sub-criteria, whereas VIKOR approach has been utilized to evaluate the environmental performance of 4 CMs and to select the most efficient one. Results show that "Ensuring easy maintenance and repair," "Improving durability and higher reliability," and "Using alternative manufacturing techniques" are the top 3 criteria for the selection of sustainable CM. In addition, CM3 stands out to be the most sustainable among the four alternative CMs because of the ability to consider key environmental criteria especially during the selection of raw materials and manufacturing processes. The outcomes of this research may be utilized by the OEMs to understand the different criteria for selection of a sustainable contract manufacturer. Also, the proposed approach can lead the OEMs to evaluate the environmental performance of different contract manufacturers and to select the best one.</p>
2.	<p><a href="#"><u>A novel strategy to enhance the cooling effectiveness in a confined porous jet impingement using non-Newtonian fluids</u></a>  PP Singh, M Trivedi, T Mondal, N Nirmalkar - International Communications in Heat and Mass Transfer, 2021</p> <p><b>Abstract:</b> Jet impingement configuration is commonly employed in the thermal management of the gas turbine engines, rocket launchers, and high-density electrical equipment cooling to remove a large amount of heat. Owing to such overwhelming applications, significant research efforts have been devoted to enhance the cooling performance of jet impingement configuration. In this work, the influence of shear-thinning behaviour in overall heat transfer characteristics have been investigated as a function of pertinent dimensionless numbers as <math>10^{-6} \leq Da \leq 10^{-2}</math> (Darcy number), <math>1 \leq Pe \leq 10^2</math> (Péclet number), <math>0 \leq Ri \leq 4</math> (Richardson number), <math>0.4 \leq n \leq 1</math> (shear-thinning index). The numerical results on local thermal non-equilibrium (LTNE) parameter, streamlines and isotherms, local and average Nusselt number are reported for a range of power-law index, Péclet number and Richardson number. All in all,</p>

	shear-thinning fluids offer 50–60% enhancement in Nusselt number with reference to the Newtonian fluid at a higher Darcy number. A correlation for average Nusselt number is put forward to enable its use for process design calculations.
3.	<p><a href="#">A simplified subsurface soil salinity estimation using synergy of SENTINEL-1 SAR and SENTINEL-2 multispectral satellite data, for early stages of wheat crop growth in Rupnagar, Punjab, India</a>  A Tripathi, R Tiwari - Land Degradation and Development, 2021</p> <p><b>Abstract:</b> Soil salinity has become a highly disastrous phenomenon responsible for crop failure worldwide, especially in countries with low farmer incomes and food insecurity. Soil salinity is often due to water accumulation in fields caused by improper flood irrigation whereby plants take up the water leaving salts behind. It is, however, the subsurface soil salinity that affects plant growth. This soil salinity prevents further water intake. There have been very few studies conducted for subsurface soil salinity estimation. Therefore our study aimed to estimate subsurface soil salinity (at 60 cm depth) for the early stage of wheat crop growth in a simplified manner using freely available satellite data, which is a novel feature and prime objective in this study. The study utilises SENTINEL-1 SAR (synthetic aperture RADAR) data for backscatter coefficient generation, SENTINEL-2A multispectral data for NDSI (normalised differential salinity index) generation and on-ground equipment for direct collection of soil electrical conductivity (EC). The data were collected for two dates in November and December 2019 and one date in January 2020 during the early stage of wheat crop growth. The dates were selected keeping in mind the satellite pass over the study area of Rupnagar on the same day. Ordinary least squares regression was used for modelling which gave R<sup>2</sup>-statistics of 0.99 and 0.958 in the training and testing phase and root mean square error (RMSE) of 1.92 and mean absolute error (MAE) of 0.78 in modelling for soil salinity estimation.</p>
4.	<p><a href="#">Analysis of Discharge Gap using Controlled RC based Circuit in <math>\mu</math>EDM Process</a>  S Raza, R Nadda, CK Nirala - Journal of The Institution of Engineers (India): Series C, 2021</p> <p><b>Abstract:</b> Owing to the dependency of real-time inter-electrode gap (discharge gap) on instantaneous discharge voltage in a resistance–capacitance (RC) circuit-based <math>\mu</math>EDM, analyzing machining responses with respect to the discharge gap could be a crucial task. This work aims to extract the information on the material removal rate (MRR) and overcut at various discharge gaps, set in terms of open-circuit voltage (<math>V_o</math>) in a controlled RC-based <math>\mu</math>EDM setup. The results have been obtained for MRR and overcut and found to be in good agreement with logical reasoning. The results have been further supported by a thorough discussion in the context of the discharge gap and corresponding discharge energy. A DAQ system has been used to capture the real-time discharge voltage data and corresponding amperage at a high sampling rate to estimate the discharge energy.</p>
5.	<p><a href="#">Anticipating response function in gene regulatory networks</a>  P Gautam, SK Sinha - Journal of the Royal Society Interface, 2021</p> <p><b>Abstract:</b> The origin of an ordered genetic response of a complex and noisy biological cell is intimately related to the detailed mechanism of protein–DNA interactions present in a wide variety of gene regulatory (GR) systems. However, the quantitative prediction of genetic response and the correlation between the mechanism and the response curve is poorly understood. Here, we report in silico binding studies of GR systems to show that the</p>

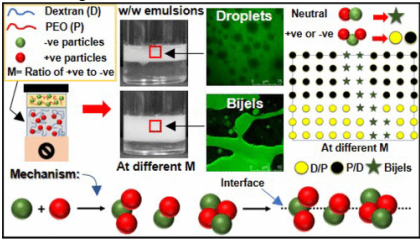
	<p>transcription factor (TF) binds to multiple DNA sites with high cooperativity spreads from specific binding sites into adjacent non-specific DNA and bends the DNA. Our analysis is not limited only to the isolated model system but also can be applied to a system containing multiple interacting genes. The controlling role of TF oligomerization, TF–ligand interactions, and DNA looping for gene expression has been also characterized. The predictions are validated against detailed grand canonical Monte Carlo simulations and published data for the lac operon system. Overall, our study reveals that the expression of target genes can be quantitatively controlled by modulating TF–ligand interactions and the bending energy of DNA.</p>
6.	<p><a href="#">Challenges, process requisites/inputs, mechanics and weld performance of dissimilar micro-friction stir welding (dissimilar <math>\mu</math>FSW): A comprehensive review</a>  M Verma, S Ahmed, P Saha - Journal of Manufacturing Processes, 2021</p> <p><b>Abstract:</b> Dissimilar micro-friction stir welding (dissimilar <math>\mu</math>FSW) can be a preferred choice for joining dissimilar materials having thickness <math>\leq 1000 \mu\text{m}</math>. The technique's potential applications are in miniaturized components, where the inherent benefits of the process, such as low temperature, low distortion, and clean joining, are advantageous compared to fusion welding. However, the challenges associated with dissimilar <math>\mu</math>FSW hinder its full potential applications in the relevant industries. The challenges are particularly a combination of two different characteristics of the process (i) the complexities of simultaneously fulfilling the dissimilar materials' demands due to the vast differences in the two materials' mechanical and thermal properties and (ii) the problems due to reduced sheet thickness. In this regard, the present work is a comprehensive and timely review of the research works done on dissimilar <math>\mu</math>FSW targeted at easily acquainting the research community about the know-how and the state of the art of the process. The review is broadly divided into three crucial parts: the process inputs/requisites, process mechanics, and process performance. The details about the <math>\mu</math>FSW tool, process parameters, and relative sheet positioning are discussed under the heading process inputs/requisites. Concerning the process mechanics, the intermetallic compound formation, defect generation, and material mixing are discussed. The joints' resulting performance is shown by detailing the essential properties such as formability, residual stresses, fatigue, hardness, and tensile strength. Additionally, several future research directions are presented at the end of this critical review to motivate further improvements in this joining technique and instigate its utility in relevant industries.</p>
7.	<p><a href="#">DeepDoT: Deep Framework for Detection of Tables in Document Images</a>  M Singh, P Goyal - International Conference on Computer Vision and Image Processing: Part of the Communications in Computer and Information Science book series, 2021</p> <p><b>Abstract:</b> An efficient table detection process offers a solution for enterprises dealing with automated analysis of digital documents. Table detection is a challenging task due to low inter-class and high intra-class dissimilarities in document images. Further, the foreground-background class imbalance problem limits the performance of table detectors (especially single stage table detectors). The existing table detectors rely on a bottom-up scheme that efficiently captures the semantic features but fails in accounting for the resolution enriched features, thus, affecting the overall detection performance. We propose an end to end trainable framework (DeepDoT), which effectively detect the tables (of different sizes) over arbitrary scales in document images. The DeepDoT utilizes a top-down as well as a bottom-up approach, and additionally, it uses focal loss for handling the pervasive class imbalance problem for accurate</p>

	<p>predictions. We consider multiple benchmark datasets: ICDAR-2013, UNLV, ICDAR-2017 POD, and MARMOT for a thorough evaluation. The proposed approach yields comparatively better performance in terms of F1-score as compared to state-of-the-art table detection approaches.</p>
8.	<p><a href="#">Depression Intensity Estimation via Social Media: A Deep Learning Approach</a> S Ghosh, T Anwar - IEEE Transactions on Computational Social Systems, 2021</p> <p><b>Abstract:</b> Depression has become a big problem in our society today. It is also a major reason for suicide, especially among teenagers. In the current outbreak of coronavirus disease (COVID-19), the affected countries have recommended social distancing and lockdown measures. Resulting in interpersonal isolation, these measures have raised serious concerns for mental health and depression. Generally, clinical psychologists diagnose depressed people via face-to-face interviews following the clinical depression criteria. However, often patients tend to not consult doctors in their early stages of depression. Nowadays, people are increasingly using social media to express their moods. In this article, we aim to predict depressed users as well as estimate their depression intensity via leveraging social media (Twitter) data, in order to aid in raising an alarm. We model this problem as a supervised learning task. We start with weakly labeling the Twitter data in a self-supervised manner. A rich set of features, including emotional, topical, behavioral, user level, and depression-related n-gram features, are extracted to represent each user. Using these features, we train a small long short-term memory (LSTM) network using Swish as an activation function, to predict the depression intensities. We perform extensive experiments to demonstrate the efficacy of our method. We outperform the baseline models for depression intensity estimation by achieving the lowest mean squared error of 1.42 and also outperform the existing state-of-the-art binary classification method by more than 2% of accuracy. We found that the depressed users frequently use negative words such as stress and sad, mostly post during late nights, highly use personal pronouns and sometimes also share personal events.</p>
9.	<p><a href="#">Design and Analysis of Aerial-Terrestrial Network: A Joint Solution for Coverage and Rate</a> D Saluja, R Singh, K Choi, S Kumar - IEEE Access, 2021</p> <p><b>Abstract:</b> The exploitation of aerial base stations (A-BSs) in conjunction with terrestrial base stations (T-BSs) is envisioned as a promising solution to provide connectivity to devices and user-equipment (UE) in crowded situations (viz. in the sports event) and emergency situations (viz. in the disaster management). However, the use of A-BSs with existing terrestrial networks intensifies the inter-cell interference (ICI) to the devices and UEs, therefore leading to a degraded signal-to-interference-ratio (SIR). This paper addresses this issue by exploiting different radio access technology (RAT) (mmWave/microwave) for aerial and terrestrial networks. Indeed, the network connectivity is always a top priority for all applications. However, there are also some applications such as remote patient monitoring, and remote working, which requires both coverage and high data-rates. But, most of the existing research claims the trade-off between the coverage and the data-rate performance. Whereas this paper aims to improve coverage and rate simultaneously in an aerial-terrestrial networks by employing an optimal combination of mmWave and microwave RAT based on the proposed association strategy. The essential analysis of such an integrated network involves the evaluation of parameters based on the analytic model. Hence, this paper analytically obtains the coverage probability (CP) and average rate expressions for the proposed integrated aerial-terrestrial networks. The analysis is</p>

	supported by probabilistic models-based simulations that agree closely with analytical results. The results claim that the proposed model leads to improved performance in terms of both CP and average rate. Also, the paper provides parametric analysis for CP and rate with A-BSs height and A-BSs density to enable its practical implementation in 5G/6G technologies
10.	<p><a href="#">Design and Development of the Automated Multimedia Device for Memorials</a> S Sharma - Recent Trends in Engineering Design: Part of the Lecture Notes in Mechanical Engineering book series, 2021</p> <p><b>Abstract:</b> The purpose of this paper is the design and development of an automated gravesite multimedia device that can be installed near the grave for paying customized tribute for deceased (humans and pets) at graveyards. This device can rise to the waist level and plays the audio–video message or information about the deceased person. The viewers can know about the history and the achievements of the deceased person. It can be used in libraries, botanical parks, national or state parks, museums, or historical sites. Most of such products are patented and similar to the serenity panel, a commercial product installed on the gravestone head. The automated gravesite multimedia device is installed near the grave. The product rises to the waist level of a person from the ground, which gives a better usage of the product. The product design process approach from specification to CAE analysis is applied.</p>
11.	<p><a href="#">Detection of slags in structural steel sample using InfraRed thermal wave imaging</a> A Rani, R Mulaveesala - Materials Today: Proceedings, 2021</p> <p><b>Abstract:</b> The estimation of defects in any material is a critical problem in the domain of InfraRed thermography (IRT). The paper presents simulation aspects of three-dimensional heat transfer model for a finite thickness structural steel sample having six different slag inclusions using a low peak power frequency modulated thermal wave imaging (FMTWI) and its digital counterpart digitized frequency modulated thermal wave imaging (DFMTWI) technique. The sample surface is subjected to proposed thermal heat flux and defect analysis was carried out by studying the thermal gradient over the test sample surface. Further, time domain pulse compression approach allowing better defect depth analysis has been discussed to evaluate the correlation coefficients and time delays for the proposed approaches. Results show better performance of the DFMTWI approach with high correlation coefficient values for all the defects with low time delays than the FMTWI approach.</p>
12.	<p><a href="#">Do macroeconomic uncertainty and financial development cause environmental degradation? Evidence from an emerging economy</a> B Rakshit, Y Neog - International Journal of Social Economics, 2021</p> <p><b>Abstract:</b> Purpose The main purpose of this paper is to empirically investigate the effect of macroeconomic uncertainty on environmental degradation in India over the period 1971–2016. Additionally, this paper considers the role of financial development, energy consumption intensity and economic growth in explaining the variation of environmental degradation in India.</p> <p>Design/methodology/approach The authors applied the power generalized autoregressive conditional heteroskedasticity model to measure inflation volatility and used it as a proxy for macroeconomic uncertainty. From a</p>



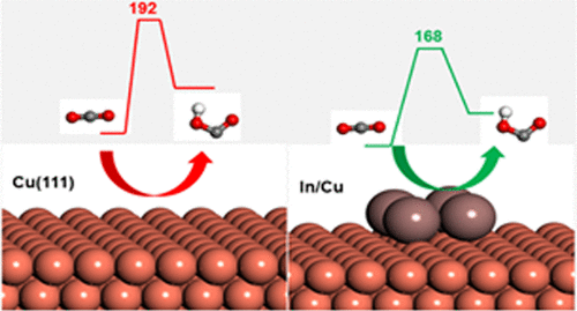
	<p>methodological perspective, the authors employ the autoregressive distributive lag bound testing model to establish the long-run equilibrium association between the variables. The Toda–Yamamoto causality approach has been used to examine the direction of causality between the variables.</p> <p><b>Findings</b> Findings suggest that macroeconomic uncertainty exerts a positive effect on carbon emissions, indicating that higher inflation volatility, as a proxy for macroeconomic uncertainty, hinders India's environmental quality. Financial development, economic growth and energy consumption intensity have also adversely impacted environmental quality.</p> <p><b>Practical implications</b> The negative association between macroeconomic uncertainty and environmental degradation calls for some stringent policy actions. While formulating policies to promote growth and maintain stability, policymakers and government stakeholders should take into account the environmental effects of macroeconomic policies. There is a need to implement more environmental-friendly technologies in the financial sector that could reduce carbon emission.</p> <p><b>Originality/value</b> To the best of the authors' knowledge, this study is the first that considers the role of macroeconomic uncertainty along with financial development and energy intensity in an emerging economy like India.</p>
13.	<p><a href="#"><u>Droplet–Bijel–Droplet Transition in Aqueous Two-Phase Systems Stabilized by Oppositely Charged Nanoparticles: A Simple Pathway to Fabricate Bijels</u></a> C Shekhar, A Kiran, V Mehandia, VR Dugyala... - Langmuir, 2021</p> <p><b>Abstract:</b> We demonstrate a novel yet straightforward methodology of stabilizing aqueous two-phase systems (ATPS) using oppositely charged nanoparticles (OCNPs). We employ commercial-grade, Ludox, OCNPs to induce self-assembly. This self-assembly route promotes the stronger adsorption of nanoparticles at the water–water interface by triggering the formation of 2D and 3D aggregates of varying sizes and shapes. The interplay of this size and shape promotes stability due to increased Gibbs detachment energy and modulates the resulting cluster adsorption at the interface, thereby the structural state of emulsions. We demonstrate the influence of polymers' and particles' composition on the structural transformation from droplet–bijel–droplet using a phase diagram. For the first time, such a structural transition and the single pathway are reported within the domain of ATPS to produce stable bijels or colloidal capsules. It is asserted that the essential condition of three-phase contact angle (<math>\theta</math>) = 90° to favor the formation of bijels can be established by selecting a suitable experimental condition using a phase diagram without employing any complicated surface modification procedures reported in the literature. Further, the mechanistic route favoring the formation of bijels and emulsion droplets at different experimental regimes is presented based on the empirical study using turbidity and zeta potential measurements. These studies reveal that the formation of bijels will be most favored when the parameter M (ratio of weight fraction of positively charged nanoparticles to negatively charged nanoparticles) is chosen between 0.7 and 4. It is intriguing to note the fact that, while the droplets stabilized by OCNPs have shown good resilience under high centrifugal action, the bijels produced in this way continued to remain stable for a long time,</p>

	<p>offering a facile route to prepare the bijels with a hierarchical bicontinuous network structure.</p> 
14.	<p><a href="#">Effect of ageing on microstructure and fracture behavior of cortical bone as determined by experiment and Extended Finite Element Method (XFEM)</a>  RN Yadav, P Uniyal, P Sihota, S Kumar, V Dhiman...N Kumar - Medical Engineering &amp; Physics, 2021</p> <p><b>Abstract:</b> Bone fracture is a severe health concern; therefore, understanding the causes of bone fracture are crucial. This paper investigates the microstructure and fracture behaviour of cadaveric cortical bone of two different groups (Young, n= 6; Aged, n=7). The microstructure is obtained from <math>\mu</math>-CT images, and the material parameters are measured with nanoindentation. Fracture behaviour in transverse and longitudinal orientations is investigated experimentally and numerically. The results show that the Haversian canal (HC) size increases and the osteon wall thickness (OWT) decreases significantly in the aged group, whereas a nonsignificant difference is found in tissue properties. The crack initiation (<math>J_{ic}</math>) and crack growth (<math>J_{grow}</math>) toughness of the aged group are found to be significantly lower (<math>p &lt; 0.01</math>) than the young group in the transverse orientation; however, for the longitudinal orientation, only the value of <math>J_{ic}</math> in the aged group is found significantly lower. Further, a 4-phase XFEM (based on micro-CT image) model is developed to investigate the crack propagation behaviour in both orientations. For the transverse orientation, results show that in the aged group, the crack initially follows the cementline and then penetrates the osteon, whereas, in the young group, it propagates along the cementline. These results are in agreement with experimental results where the decrease in <math>J_{grow}</math> is more significant than the <math>J_{ic}</math> in the aged group. This study suggests that ageing leads to a larger HC and reduced OWT, which weakens the crack deflection ability and causes fragility fracture. Further, the XFEM results indicate that the presence of a small microcrack in the vicinity of a major crack tip causes an increase in the critical stress intensity factor.</p>
15.	<p><a href="#">Effect of surface modification on mechanical properties of filature silk waste and nanoclay filler-based polymer matrix composite</a>  R Nair, A Bhattacharya, P Bhowmik, R Kant - Polymers and Polymer Composites, 2021</p> <p><b>Abstract:</b> Natural fibers have been attracting researchers and engineers as an alternative reinforcement of synthetic fibers in polymer composites due to their low cost, availability from natural resources, satisfactory high modulus and tensile strength, and biodegradability. Filature silk waste (FSW) is the remnant part of the cocoons which is produced during the silk forming process. The current study focuses on the comparison of tensile properties between untreated filature silk waste reinforced epoxy-based composite (UTFSWREC), 2 wt% alkali-treated filature silk waste reinforced epoxy-based composites (TFSWREC) and 2 wt% alkali-treated filature silk waste reinforced epoxy nanocomposites (TFSWRENC). The tensile properties showed that Young's modulus of composites increases with surface modification of fiber and further enhances with nanoclay filler. TFSWREC and TFSWRENC displayed a higher tensile</p>

	<p>modulus than UTFSWREC. Scanning Electron Microscopy (SEM) showed the removal of the sericin layer from the surface of fiber, which resulted in the separation of fibrils and further resulted in the enhancement of the mechanical properties. FTIR analysis confirmed that intermolecular bonding improves with the chemical treatment and further refined with nanoclay filler addition.</p>
16.	<p><a href="#">Effects of blockage and fluid inertia on drag and heat transfer of a solid sphere translating in FENE-P viscoelastic fluids in a tube</a>  A Chauhan, C Sasmal, RP Chhabra - Journal of Non-Newtonian Fluid Mechanics, 2021</p> <p><b>Abstract:</b> An extensive numerical investigation of the flow and heat transfer phenomena of a solid sphere translating in a cylindrical tube filled with FENE-P viscoelastic fluids is reported herein. The governing equations, namely, mass, momentum, energy, and viscoelastic constitutive equations, have been solved over the following ranges of conditions: Reynolds number, <math>1 \leq Re \leq 100</math>, Weissenberg number, <math>0 \leq Wi \leq 10</math>, polymer extensibility parameter, <math>10 \leq L^2 \leq 500</math> and blockage ratio, <math>0 \leq BR \leq 0.7</math> for a fixed value of the polymer viscosity ratio <math>\beta = 0.5</math> and Prandtl number <math>Pr = 10</math>. Limited simulations with the FENE-CR viscoelastic fluid model have also been carried out to make a comparison between the two viscoelastic models. At low Reynolds numbers, the velocity overshoot and/or negative wake downstream the sphere has been observed under appropriate conditions. This tendency of their appearing decreases with the increasing Reynolds number, and decreasing blockage ratio, polymer extensibility parameter and Weissenberg number. The size of the recirculation region (wake length) increases with the Weissenberg number at low values of the polymer extensibility parameter, whereas a reverse trend is seen at high values of <math>L^2</math>. The drag coefficient decreases with the Reynolds and Weissenberg numbers, whereas it increases with the blockage ratio. On the other hand, the average Nusselt number always increases with the Reynolds number irrespective of the values of <math>Wi</math>, <math>L^2</math> and <math>BR</math>. However, the corresponding effect of the blockage ratio and polymer extensibility parameter is seen to be more complex modulated by the values of <math>Re</math> and <math>Wi</math>. For instance, at high Reynolds numbers, the average Nusselt number always increases with the blockage ratio; however, at low values of it, there is a critical value of the blockage ratio is present up to which the average Nusselt number increases, and beyond that, it decreases. Furthermore, the average Nusselt number always initially increases up to a certain value of the Weissenberg number, and after that, it remains almost constant or decreases depending upon the values of <math>L^2</math>, <math>BR</math> and <math>Re</math>. Finally, simple correlations for the average Nusselt number and drag ratio are presented, which not only capture the functional dependence of the governing parameters, but also can be used for the interpolation of the present results for the intermediate values of the governing parameters in a new application.</p>
17.	<p><a href="#">Estimation of Endurance Coefficient of Insulating Material under Uniform and Non-Uniform Fields by Damage Equalization Method</a>  AJ Thomas, CC Reddy - IEEE Conference on Electrical Insulation and Dielectric Phenomena, 2020</p> <p><b>Abstract:</b> In high voltage insulation system, the insulation will be undergoing various stresses and the life of the insulation will be different from uniform fields when stressed by a divergent field. In this paper, dc breakdown experiments at different step stresses are conducted using needle-plane and plane-plane electrode systems. Using the data from the breakdown tests, assessment of life of the insulating material can be done by estimating the voltage endurance</p>



	<p>coefficient (n) and accumulated damage. Stepped-stress damage equalization method (SSDEM) is used for estimating the life of the insulating material used. Interesting results on the role of uniform and non-uniform field on endurance coefficient is reported which in turn shows the effect of divergent and uniform stress on the life of the insulation. Furthermore, in this study, a numerical model is developed to estimate the electric field around the tip of the needle electrode using a semi-empirical equation of nonlinear conduction under steady state DC. Spherical geometry system is used for solving the differential equations numerically. The results show the developed numerical model can predict the Poisson's field when conduction is field dependent.</p>
18.	<p><a href="#">Experimental Investigations of Alpha Particle Irradiation of Natural Nickel</a>  VV Savadi, DP Singh, A Yadav, PP Singh, MK Sharma... - Indian Journal of Pure &amp; Applied Physics, 2021</p> <p><b>Abstract:</b> Attempts have been made to measure the activity in irradiated natural Ni material induced by <math>\alpha</math>-particles in the energy range 10-40 MeV followed by stack foil activation technique. Activity induced has been determined through the cross-sections obtained from various reactions for <math>^{58}\text{Ni}(\alpha, p)^{61}\text{Cu}</math>, <math>^{58}\text{Ni}(\alpha, pn)^{60}\text{Cu}</math>, <math>^{60}\text{Ni}(\alpha, p2n)^{61}\text{Cu}</math>, <math>^{60}\text{Ni}(\alpha, n)^{63}\text{Zn}</math>, <math>^{60}\text{Ni}(\alpha, 2n)^{62}\text{Zn}</math>, <math>^{61}\text{Ni}(\alpha, 3n)^{62}\text{Zn}</math> and <math>^{61}\text{Ni}(\alpha, 2n)^{63}\text{Zn}</math> in <math>\alpha^{+nat}\text{Ni}</math> interaction at different beam energies has been found to vary from 10-26 microns.</p>
19.	<p><a href="#">Graphitic Carbon Nitride Modified with Zr-Thiamine Complex for Efficient Photocatalytic CO<sub>2</sub> Insertion to Epoxide: Comparison with Traditional Thermal Catalysis</a>  A Kumar, S Samanta, R Srivastava - ACS Applied Nano Materials, 2021</p> <p><b>Abstract:</b> CO<sub>2</sub> conversion to valuable chemicals and fuels at ambient temperature and atmospheric pressure using a sustainable energy source is an attractive but challenging task. Herein, Zr-thiamine is pyrolyzed with urea under N<sub>2</sub> atmosphere to prepare Zr-thiamine modified carbon nitride (Zr-Thia/g-CN) catalyst. The catalyst exhibits optimum Lewis acidity and basicity to produce excellent cyclic carbonate yields by the insertion reaction of CO<sub>2</sub> into epoxide on a large scale under neat conditions in the absence of any cocatalyst under traditional thermal catalysis in 6 h. The catalyst exhibits similar cyclic carbonate yield under simulated light (250 W Hg lamp, <math>\lambda &gt; 360</math> nm) in 24 h and, most importantly, under sunlight in 12 h in the presence of a low amount of cocatalyst (2.5 mol % with respect to epoxide) under ambient temperature, 1 bar pressure, and neat conditions. The catalyst is efficiently recycled up to 5 cycles in traditional thermal catalysis and photocatalytic conditions. The structure–activity relationship is established, and the reaction mechanism is proposed with the help of CO<sub>2</sub> adsorption, CO<sub>2</sub> temperature-programmed desorption techniques, acidity–basicity measurements, optoelectronic properties, control reactions, and catalytic activity data. The development of a single catalyst for catalyzing the same reaction under traditional thermal catalytic and sustainable photocatalytic conditions will attract researchers of different disciplines.</p>
20.	<p><a href="#">Highly efficient parallel algorithms for solving the Bates PIDE for pricing options on a GPU</a>  A Ghosh, C Mishra - Applied Mathematics and Computation, 2021</p> <p><b>Abstract:</b> In this paper we investigate faster and memory efficient parallel techniques to numerically solve the Bates model for European options. We have followed method-of-lines approach and implemented the numerical algorithms on a graphics processing unit (GPU). Two second order finite difference (FD) schemes are taken into account that yield discretization matrices with tridiagonal and pentadiagonal block structures. Three recent adaptations of an alternating direction implicit scheme are employed for time-stepping. Spatial and temporal errors</p>

	<p>corresponding to our chosen FD and time-stepping schemes are numerically studied. For parallel computation of solutions we have applied the well-know parallel cyclic reduction (PCR) algorithm for tridiagonal systems and our novel PCR algorithm for pentadiagonal systems. Ample numerical experiments are performed to study speed and accuracy on three platforms: single GPU using CUDA, multi-core CPU using OpenMP and an efficient sequential algorithm on a single core using MATLAB, where substantial speed-up is observed on the GPU. Sensitivities of computational times of the sequential algorithm in MATLAB with respect to certain parameters in the Bates model are also analysed.</p>
21.	<p><a href="#">High-resolution digital spatial control of a highly multimode laser</a> C Tradonsky, S Mahler, G Cai, V Pal, R Chriki... - Optica, 2021</p> <p><b>Abstract:</b> We developed a rapid and efficient method for generating laser outputs with arbitrary shaped distributions and properties that are needed for a variety of applications. It is based on simultaneously controlling the intensity, phase, and coherence distributions of the laser. The method involves a digital degenerate cavity laser in which a phase-only spatial light modulator and spatial filters are incorporated. As a result, a variety of unique and high-resolution arbitrary shaped laser beams were generated with either a low or a high spatial coherence and with a minimal change in the laser output power. By controlling the phase, intensity, and coherence distributions, a shaped laser beam was efficiently reshaped into a completely different shape after free space propagation. The generation of such laser beams could lead to new and interesting applications.</p>
22.	<p><a href="#">Influence of Indium as a Promoter on the Stability and Selectivity of the Nanocrystalline Cu/CeO<sub>2</sub> Catalyst for CO<sub>2</sub> Hydrogenation to Methanol</a> SK Sharma, B Paul, RS Pal, P Bhanja, A Banerjee... - ACS Applied Materials &amp; Interfaces, 2021</p> <p><b>Abstract:</b> Stable catalyst development for CO<sub>2</sub> hydrogenation to methanol is a challenge in catalysis. In this study, indium (In)-promoted Cu nanoparticles supported on nanocrystalline CeO<sub>2</sub> catalysts were prepared and explored for methanol production from CO<sub>2</sub>. In-promoted Cu catalysts with ~1 wt % In loading showed a methanol production rate of 0.016 mol gCu<sup>-1</sup> h<sup>-1</sup> with 95% methanol selectivity and no loss of activity for 100 h. It is found that the addition of indium remarkably increases Cu dispersion and decreases Cu particle size. In addition led to an increased metal–support interaction, which stabilizes Cu particles against sintering during the reaction, leading to high stability and activity. In addition, density functional theory calculations suggested that the reaction is proceeding via reverse water gas shift (RWGS) mechanism where the presence of In stabilized intermediate species and lowered CO<sub>2</sub> activation energy barriers.</p> 

[InfraRed Image Correlation for Non-destructive Testing and Evaluation of Delaminations in Glass Fibre Reinforced Polymer Materials](#)

G Dua, R Mulaveesala, P Mishra - Infrared Physics & Technology, 2021

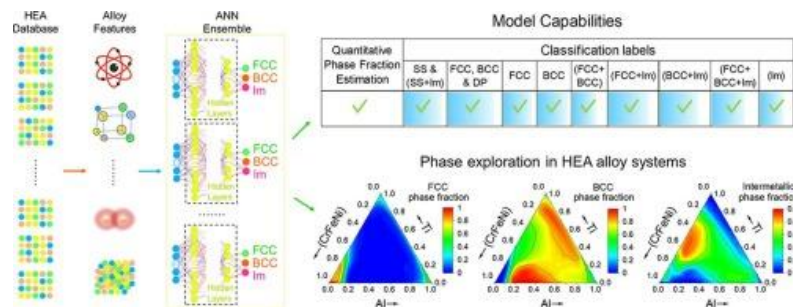
23. **Abstract:** InfraRed Thermography (IRT) is one of the widely used Non-destructive Testing and Evaluation (NDT&E) method for characterization of fiber reinforced polymers. Among verity of testing methodologies and associated post processing schemes recently proposed pulse compression favorable thermal wave imaging methodologies gain importance due to their merits. This present paper highlights a highly depth resolved Frequency Modulated Thermal Wave Imaging (FMTWI) and its digitized version named as Digitized Frequency Modulated Thermal Wave Imaging (DFMTWI) for identification of subsurface Teflon patches introduced as defects to simulate the delaminations at various layers of GFRP test specimen of various sizes and depths.

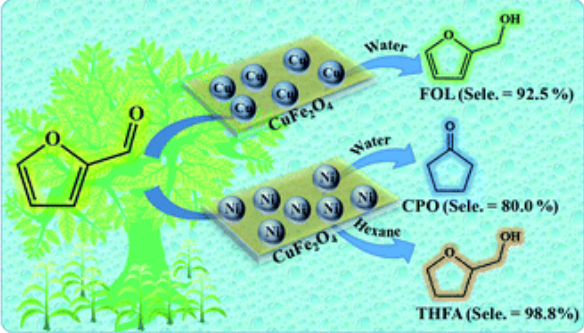
[Learning phase selection and assemblages in High-Entropy Alloys through a stochastic ensemble-averaging model](#)

D Beniwal, PK Ray - Computational Materials Science, 2021

24. **Abstract:** Efficient alloy design requires a knowledge of phase selection, phase-fractions and microstructure of the material. Prediction of the phase equilibria, though well-established for traditional alloys, is still an open challenge for novel materials and concentrated multicomponent systems such as the High-Entropy Alloys (HEAs). In this paper, we present a novel data-driven approach for learning the phase-equilibria in HEAs through the use of a stochastic ensemble averaging method. The proposed model employs a model-averaging technique on an ensemble of 150 artificial neural networks that have been trained on a 323 alloy dataset. A seven-label classification is presented using a three-element vector description of phases. This allows us to fit the classification boundaries to a relatively larger number of phase combination labels while using only three target parameters for training thereby improving accuracy. The phase prediction capabilities (i.e., formation of FCC, BCC, intermetallics or different combinations of these phases) were tested on 320 alloys outside of the training dataset. Additionally, quantitative estimate of the phase equilibria, i.e., relative phase-fractions, were estimated and compared with experimental measurements and CALPHAD predictions in three different high-entropy systems, viz.,  $\text{Fe}_x\text{-Ni}_y\text{-(AlCoCr}_{0.5})_{1-x-y}$ ,  $\text{Al}_x\text{-Ti}_y\text{-(CrFeNi)}_{1-x-y}$  and  $\text{Cr}_x\text{-Mo}_y\text{-(VNbTi)}_{1-x-y}$ . The model's capability of going a step beyond current state-of-the-art model allows greater insights into target composition spaces for the alloy designer and establishes the first such approach for HEAs.

**Graphical Abstract:**



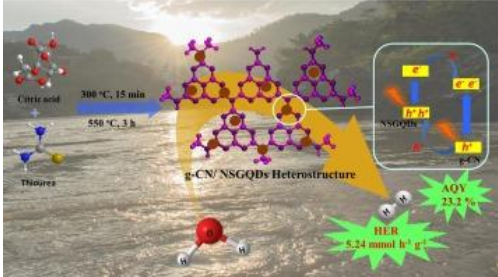
25.	<p><a href="#">Mechanical Properties of the Ti<sub>2</sub>AlNb Intermetallic: A Review</a>  K Goyal, N Sardana - Transactions of the Indian Institute of Metals, 2021</p> <p><b>Abstract:</b> Ti<sub>2</sub>AlNb intermetallics are promising next-generation aerospace materials. Advancement in non-conventional manufacturing methods has made the fabrication of these intermetallics economical. However, post-heat treatments are required to obtain desired mechanical properties, which further depend on the microstructural features of the intermetallics. Extensive studies have been conducted to understand the relation between mechanical behavior and microstructural features of this intermetallic. This review presents the effect of various microstructural features of (a) fully B2 and <math>\alpha_2</math> + B2, (b) fully lamellar, (c) bimodal lamellar, (d) equiaxed and duplex, and (e) plate-like O phase on room temperature properties, namely strength, ductility, and fracture mechanisms. Moreover, the review emphasizes the special microstructural features that are required to enhance the mechanical properties of the alloy.</p>
26.	<p><a href="#">Metal and solvent-dependent activity of spinel-based catalysts for the selective hydrogenation and rearrangement of furfural</a>  A Kumar, A Shivhare, R Bal, R Srivastava - Sustainable Energy &amp; Fuels, 2021</p> <p><b>Abstract:</b> The development of cost-effective heterogeneous catalysts for the selective conversion of biomass-derived platform chemicals into value-added chemicals and liquid fuels will pave the way towards the development of sustainable biorefineries. Herein, we perform in-depth optimization of the catalyst composition and experimental conditions to selectively produce three important value-added chemicals from furfural, including cyclopentanone, furfuryl alcohol, and tetrahydrofurfuryl alcohol. Results show that the Ni(10%)/CuFe<sub>2</sub>O<sub>4</sub> catalyst affords cyclopentanone as a major product with &gt;90% selectivity in water at 423 K and 1 MPa H<sub>2</sub>. Meanwhile, switching to non-aqueous solvents, including hexane, isopropanol, toluene, and ethanol, selectively produces tetrahydrofurfuryl alcohol as a major product under identical reaction conditions. Over the Cu(10%)/CuFe<sub>2</sub>O<sub>4</sub> catalyst, furfuryl alcohol is produced as a major product in water at 393 K and 1 MPa H<sub>2</sub>. Control experiments over M/CuO, M/Fe<sub>3</sub>O<sub>4</sub>, and M/SBA-15 catalysts are also performed; however, these catalysts afford much lower conversion compared to the M/CuFe<sub>2</sub>O<sub>4</sub> catalysts due to the higher Lewis acidity of the CuFe<sub>2</sub>O<sub>4</sub> support. The physicochemical properties of these catalysts are characterized using powder XRD, HR-TEM, XPS, and pyridine FT-IR. Finally, based on the existing literature, plausible reaction mechanisms for the production of cyclopentanone, tetrahydrofurfuryl alcohol, and furfural alcohol on M/CuFe<sub>2</sub>O<sub>4</sub> catalysts are proposed. The present work provides insight into the development of cost-effective and efficient catalysts for the valorization of furfural under mild conditions.</p> 

27.	<p><a href="#">Microfluidic synthesis of platinum nanoparticles supported on reduced graphene oxide, titanium dioxide, and carbon for PEM fuel cells</a>  SP Gumfekar, SH Sonawane, PL Suryawanshi - The Canadian Journal of Chemical Engineering, 2021</p> <p><b>Abstract:</b> Platinum (Pt) nanoparticles on various supports, such as commercial carbon powder, titanium dioxide (TiO<sub>2</sub>), and reduced graphene oxide (rGO), were synthesized using a continuous flow microfluidic system. First, the support materials were separately synthesized using the sonochemical technique followed by the loading of Pt. The Pt nanoparticles on different supports were characterized using Brunauer–Emmett–Teller (BET) for surface area and porosity analysis; X-ray diffraction (XRD) for structural confirmation; Fourier transform infrared (FTIR) spectroscopy and X-ray photoelectron spectroscopy (XPS) for surface composition; and transmission electron microscopy (TEM) for morphological investigation. Further, polymer electrolyte membrane (PEM) fuel cells were fabricated using the Pt nanoparticles on different supports, and cyclic voltammetry (CV), linear sweep voltammetry (LSV), and power density were performed. Among the three electrocatalysts, Pt/rGO showed the highest electrochemical performance. Pt/rGO showed higher specific activity (119 mA/cm<sup>2</sup>), mass activity (238 mA/mg), current density (1274 mA/cm<sup>2</sup>), and power density (497 mW/cm<sup>2</sup>). We also determined the mass activity and specific activity of the electrocatalysts based on the electrochemical data. This work shows the potential of the microfluidic system to continuously synthesize the technologically important nanomaterials and their application for energy conversion devices.</p>
28.	<p><a href="#">Network synchronization, stability and rhythmic processes in a diffusive mean-field coupled SEIR model</a>  T Verma, AK Gupta - Communications in Nonlinear Science and Numerical Simulation, 2021</p> <p><b>Abstract:</b> Connectivity and rates of movement have profound effect on the persistence and extinction of infectious diseases. The emerging disease spread rapidly, due to the movement of infectious persons to some other regions, which has been witnessed in case of novel coronavirus disease 2019 (COVID-19). So, the networks and the epidemiology of directly transmitted infectious diseases are fundamentally linked. Motivated by the recent empirical evidence on the dispersal of infected individuals among the patches, we present the epidemic model SEIR (Susceptible-Exposed-Infected-Recovered) in which the population is divided into patches which form a network and the patches are connected through mean-field diffusive coupling. The corresponding unstable epidemiology classes will be synchronized and achieve stable state when the patches are coupled. Apart from synchronization and stability, the coupled model enables a range of rhythmic processes such as birhythmicity and rhythmogenesis which have not been investigated in epidemiology. The stability of Disease Free Equilibrium (or Endemic Equilibrium) is attained through cessation of oscillation mechanism namely Oscillation Death (OD) and Amplitude Death (AD). Corresponding to identical and non-identical epidemiology classes of patches, the different steady states are obtained and its transition is taking place through Hopf and transcritical bifurcation.</p>



29.	<p><a href="#"><u>Noble metal-free Cu (I)-anchored NHC-based MOF for highly recyclable fixation of CO<sub>2</sub> under RT and atmospheric pressure conditions</u></a>  R Das, CM Nagaraja - Green Chemistry, 2021</p> <p><b>Abstract:</b> The utilization of CO<sub>2</sub> as C1 feedstock for synthesis of high-value chemicals and fuels is an important step towards mitigating the increasing concentration of atmospheric carbon dioxide as well as production of value-added chemicals. Herein, we demonstrate development of an efficient recyclable catalyst for conversion of CO<sub>2</sub> into oxazolidinones, important commodity chemicals for antibiotics by utilizing an N-heterocyclic carbene (NHC)-based MOF. The NHC-centers lined in the pore walls of the MOF were utilized to anchor catalytically active Cu(I) ions by post-synthetic modification (PSM). The Cu(I)-embedded MOF showed highly recyclable and selective CO<sub>2</sub> uptake property with a high heat of interaction energy of 43 kJmol<sup>-1</sup>. The presence of high density of CO<sub>2</sub>-philic NHC and catalytic Cu(I) sites in the 1D channels of the MOF render highly efficient catalytic activity for fixation of CO<sub>2</sub> into <math>\alpha</math>-alkylidene cyclic carbonates and oxazolidinones at RT and atmospheric pressure conditions. Notably, the Cu(I)@NHC-MOF showed excellent recyclability for up to 10 cycles of regeneration with retention of catalytic activity as well as chemical stability. To the best of our knowledge, Cu(I)@NHC-MOF is the first example of a noble metal-free MOF-based heterogeneous catalyst for utilization of CO<sub>2</sub> to synthesize important value-added chemicals under mild conditions.</p>
30.	<p><a href="#"><u>Numerical Investigation of Swirl and Tumble Motion in the Cylinder and Their Effect on Combustion of Gasoline–Methanol Blends in SI Engine</u></a>  NK Yadav, RK Maurya - Advances in Fluid and Thermal Engineering: Part of the Lecture Notes in Mechanical Engineering book series, 2021</p> <p><b>Abstract:</b> Two-wheeler vehicles are having challenges in adopting advanced after-treatment devices due to their compactness and lightweight. Swirl and tumble motion inside the cylinder is considered to be the desired way to improve combustion efficiency and reduce engine emissions. The present study investigates the effect of swirl and tumble motion on combustion characteristics of gasoline–methanol blend in the SI engine. This study presents a new approach to calculate the motion of the flow, including swirl and tumble during both the intake and the compression strokes using 3D-CFD simulation. The effects of the swirl and tumble variations were evaluated in terms of the swirl and tumble ratios, the turbulent kinetic energy, and the vortex motion characteristics at intake valve closing (IVC). The numerical simulations are conducted at different engine speed, and the effect of engine speeds on the in-cylinder fluid motions are analyzed and presented. Four different methanol–gasoline blends (M05, M10, M15, and M20) are used to investigate the effect of different blends on engine performance and emission. A model of 2D cylinder piston cavity is used for combustion simulation at different speeds of the engine for different swirl and tumble ratios. It was found that the swirl and tumble ratios mainly vary with the position of crank angle. The cylinder pressure increases with the increase in methanol percentage. Additionally, the turbulent kinetic energy increases with the increase of speed and swirl and tumble ratio, which leads to the completeness of combustion and improves the performance of the engine.</p>

31.	<p><a href="#"><u>Proposal for energy efficient spin transfer torque-magnetoresistive random access memory device</u></a>  A Sharma, AA Tulapurkar, B Muralidharan - Journal of Applied Physics, 2021</p> <p><b>Abstract:</b> Utilizing the electronic analogs of optical phenomena such as anti-reflection coating and resonance for spintronic devices, we propose and theoretically analyze the design of a spin transfer torque-magnetoresistive random access memory (STT-MRAM) device. The proposed device consists of a superlattice heterostructure terminated with the anti-reflective regions sandwiched between the fixed and free ferromagnetic layers. Employing Green's function spin-transport formalism coupled self-consistently with the stochastic Landau–Lifshitz–Gilbert–Slonczewski equation, we design an STT-MRAM based on the anti-reflective superlattice magnetic tunnel junction (AR-SLMTJ) device having an ultrahigh tunnel magnetoresistance (<math>\approx 3.5 \times 10^4\%</math>) and large spin current. We demonstrate that the STT-MRAM based on the AR-SLMTJ structure owing to the physics of bandpass spin filtering is nearly 1100% more energy efficient than trilayer magnetic tunnel junction (MTJ) based STT-MRAM. We also present detailed probabilistic switching and energy analysis to find out the optimal point of operation of a trilayer MTJ and AR-SLMTJ based STT-MRAM. Our predictions serve as a template to consider the heterostructures for next-generation spintronic device applications.</p>
32.	<p><a href="#"><u>Quantification of thermal energy generation in annular hyperbolic porous-finned heat sinks using inverse optimization</u></a>  S Pal, R Das - Proceedings of the Institution of Mechanical Engineers, Part E: Journal of Process Mechanical Engineering, 2021</p> <p><b>Abstract:</b> The present paper introduces an accurate numerical procedure to assess the internal thermal energy generation in an annular porous-finned heat sink from the sole assessment of surface temperature profile using the golden section search technique. All possible heat transfer modes and temperature dependence of all thermal parameters are accounted for in the present nonlinear model. At first, the direct problem is numerically solved using the Runge–Kutta method, whereas for predicting the prevailing heat generation within a given generalized fin domain an inverse method is used with the aid of the golden section search technique. After simplifications, the proposed scheme is credibly verified with other methodologies reported in the existing literature. Numerical predictions are performed under different levels of Gaussian noise from which accurate reconstructions are observed for measurement error up to 20%. The sensitivity study deciphers that the surface temperature field in itself is a strong function of the surface porosity, and the same is controlled through a joint trade-off among heat generation and other thermo-geometrical parameters. The present results acquired from the golden section search technique-assisted inverse method are proposed to be suitable for designing effective and robust porous fin heat sinks in order to deliver safe and enhanced heat transfer along with significant weight reduction with respect to the conventionally used systems. The present inverse estimation technique is proposed to be robust as it can be easily tailored to analyse all possible geometries manufactured from any material in a more accurate manner by taking into account all feasible heat transfer modes.</p>

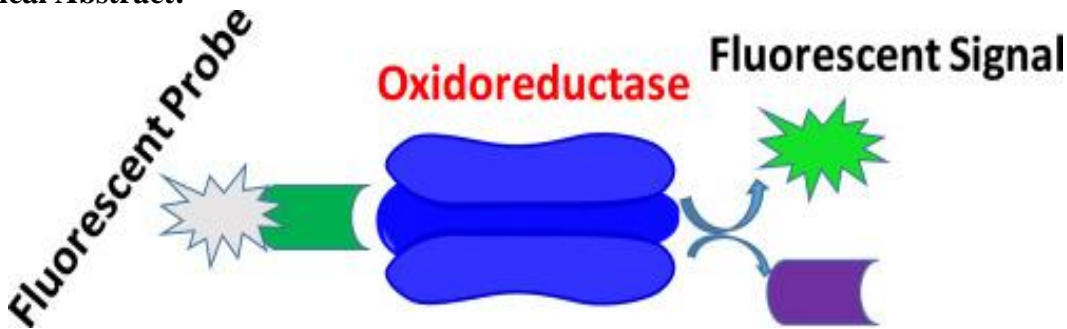
33.	<p><a href="#">Solar driven photocatalytic hydrogen evolution using graphitic-carbon nitride/NSGQDs heterostructures</a>  S Samanta, VR Battula, N Sardana, K Kailasam - Applied Surface Science, 2021</p> <p><b>Abstract:</b> The evolution of hydrogen by splitting water and sunlight renders a promising approach to produce scalable and sustainable carbon-free green energy. In this aspect, development of semiconductor heterostructure photocatalyst can spatially separate photogenerated electron-hole at the heterojunction interface and inhibit charge recombination to synergistically enhance photocatalytic performance. Herein, for the first time, we have designed exfoliated graphitic-carbon nitride (g-CN)/N, S co-doped graphene quantum dots (NSGQDs) heterostructure grown by one pot pyrolysis process. NSGQDs create strong <math>\pi</math>-<math>\pi</math> interactions with g-CN to construct an effective heterostructure and thus act as a efficient photosensitizer. We have made extensive investigations to understand the nature of g-CN/NSGQDs heterostructure, like optical and electrochemical properties and its shows improved charge transfer kinetics with reduced recombination. As a result, g-CN/NSGQDs heterostructure has achieved significantly high hydrogen evolution rate (HER) of <math>5.24 \text{ mmol h}^{-1} \text{ g}^{-1}</math> under sunlight and with the apparent quantum yield (AQY) of 23.2%.</p> <p><b>Graphical Abstract:</b> NSGQDs photosensitizer deposition over the g-CN surface (g-CN/NSGQDs heterostructure) charges distribution and improve the electron transfer kinetics and utilize solar light to enhance hydrogen evolution rate through photocatalytic water splitting.</p> 
34.	<p><a href="#">Stability criteria and convective mass transfer from the falling spherical drops, part I: Bingham plastic fluids</a>  N Nirmalkar, MJ Alam, AK Gupta - The Canadian Journal of Chemical Engineering</p> <p><b>Abstract:</b> This work deals with the flow and mass transfer around a falling spherical drop in Bingham plastic fluids. Bubbles, drops, and particles are often dispersed in a suspending fluid of non-Newtonian nature. For example, suspensions of particles in a polymer solution are used in hydraulic fracturing slurries and swarms of bubbles are used in airlift bioreactors containing various biomacromolecules, as well as in foam production, degassing, and de-volatilization of polymer melts. Governing equations for momentum and mass transfer and the Bingham constitutive equation are solved over a wide range of dimensionless groups as Reynolds number, <math>1 \leq \text{Re} \leq 150</math>; Schmidt number, <math>1 \leq \text{Sc} \leq 100</math>; Bingham number, <math>0 \leq \text{Bn} \leq 50</math>; and viscosity ratio (0.1 and 10). The local underline transport processes are expressed using streamlines, concentration contours, and sheared and un-sheared regions, whereas the average transport quantities are reported in terms of drag coefficient, critical yield-stress parameter, and Sherwood number. A co-existence of sheared and unsheared regions occurs within the flow domain due to the fluid-yield stress. The sheared regions progressively diminish with the increasing value of the</p>

	<p>Bingham number. On the other hand, inertial effects (increasing <math>Re</math>) promotes the expansion of the sheared region in the flow domain. The new modified dimensionless groups are defined by re-scaling the governing equations based on the effective viscosity of the fluid. Finally, the present numerical values of the drag and average Sherwood number are correlated using the new modified dimensionless numbers.</p>
35.	<p><a href="#">Strain effect on topological and thermoelectric properties of half Heusler compounds XPtS (X= Sr, Ba)</a>  A Yadav, S Kumar, M Muruganathan, R Kumar - Journal of Physics: Condensed Matter, 2021</p> <p><b>Abstract:</b> In this article, we report theoretical investigations of topological and thermoelectric properties of non-centrosymmetric half Heusler compounds XPtS (<math>X = \text{Sr, Ba}</math>) using first principles calculations. In addition, we also investigated the effect of static strain (up to 10%) on its topological and thermoelectric properties. Our detailed investigations show that the XPtS compounds are topological insulators and continue as topological insulators up to a strain of 10%. However, the band gap becomes a maximum of 0.213 eV under a strain of 3% for SrPtS and 0.164 eV at a strain of 5% for BaPtS. Thermoelectric investigations show that the value of merit (a measure of thermoelectric performance) <math>ZT</math> becomes maximum (0.222) at room temperature for BaPtS under a strain of 1%. The detailed theoretical investigations of XPtS with and without strain provide a theoretical platform for experiments and its possible applications in spintronics and thermoelectricity.</p>
36.	<p><a href="#">Strain modulation for enhancing Cu–Zn ordering in CZTS absorber layer using seed layer assisted growth for efficient carrier transport</a>  K Kaur, A Ghosh, Nisika, M Kumar - Applied Physics Letters, 2021</p> <p><b>Abstract:</b> <math>\text{Cu}_2\text{ZnSnS}_4</math> (CZTS) solar cells suffer from lower power conversion efficiency relative to its fellow copper indium gallium selenide thin-film technology, which have been asserted on the existence of non-stoichiometry and high degree of Cu–Zn disorder. Huge disparity among the lattice constants of Mo and CZTS is one of the causes of inducing strain in the film, which often creates defects in the CZTS structure. This work focused on investigating the effect of strain modulation using seed layer (SL) assisted growth on the structural and optoelectronic properties of CZTS films. The results indicate that SL growth of CZTS reduces strain in the film and improves the crystallinity and overall quality of the CZTS absorber, as indicated by SEM and x-ray diffraction studies. Raman shifts to higher wavenumber and photoluminescence (PL) energy shift corresponding to dominant band-to-band transition in SL CZTS correlate perfectly with the high value of order parameter. Bandgap enhancement and reduction in the Urbach energy of SL CZTS implicate higher ordering (reduction in Cu–Zn disorder) due to strain modulation. Consequently, substantial improvement from 2.13 to 13.5 <math>\text{cm}^2/\text{Vs}</math> in hole mobility is achieved. Finally, the faster response of the photodetector based on SL CZTS compared to without SL growth supports all the findings. Our results imply that SL assisted growth of CZTS could be critical to obtain a high-quality CZTS absorber layer.</p>
37.	<p><a href="#">Structural Analysis of Wikigraph to Investigate Quality Grades of Wikipedia Articles</a>  A Chhabra, S Srivastava, SRS Iyengar... - Companion Proceedings of the Web Conference, 2021</p> <p><b>Abstract:</b> The quality of Wikipedia articles is manually evaluated which is time inefficient as well as susceptible to human bias. An automated assessment of these articles may help in</p>

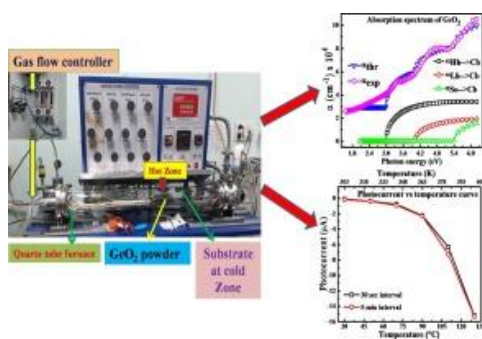
	<p>minimizing the overall time and manual errors. In this paper, we present a novel approach based on the structural analysis of Wikigraph to automate the estimation of the quality of Wikipedia articles. We examine the network built using the complete set of English Wikipedia articles and identify the variation of network signatures of the articles with respect to their quality. Our study shows that these signatures are useful for estimating the quality grades of un-assessed articles with an accuracy surpassing the existing approaches in this direction. The results of the study may help in reducing the need for human involvement for quality assessment tasks.</p>
38.	<p><a href="#">Tracing the Factoids: the Anatomy of Information Re-organization in Wikipedia Articles</a>  AA Verma, N Dubey, SRS Iyengar, S Setia - Companion Proceedings of the Web Conference 2021, 2021</p> <p><b>Abstract:</b> Wikipedia articles are known for their exhaustive knowledge and extensive collaboration. Users perform various tasks that include editing in terms of adding new facts or rectifying some mistakes, looking up new topics, or simply browsing. In this paper, we investigate the impact of gradual edits on the re-positioning and organization of the factual information in Wikipedia articles. Literature shows that in a collaborative system, a set of contributors are responsible for seeking, perceiving, and organizing the information. However, very little is known about the evolution of information organization on Wikipedia articles. Based on our analysis, we show that in a Wikipedia article, the crowd is capable of placing the factual information to its correct position, eventually reducing the knowledge gaps. We also show that the majority of information re-arrangement occurs in the initial stages of the article development and gradually decreases in the later stages.</p> <p>Our findings advance our understanding of the fundamentals of information organization on Wikipedia articles and can have implications for developers aiming to improve the content quality and completeness of Wikipedia articles.</p>
39.	<p><a href="#">Trajectory Design for Throughput Maximization in UAV-Assisted Communication System</a>  N Gupta, S Agarwal, D Mishra - IEEE Transactions on Green Communications and Networking, 2021</p> <p><b>Abstract:</b> In this paper, we study an unmanned aerial vehicle (UAV) assisted communication system to provide service to the ground users. We address the problem of UAV deployment in three-dimensional (3D) space to provide on-demand coverage to the users such that their sum rate is maximized. First, we find the optimal UAV location in 3D space where the sum rate is maximized for all ground users. Thereafter an optimal trajectory is designed for the UAV to travel from the initial to the optimal location, such that the overall average sum rate during the flight is maximized while meeting the on-board energy availability and flight duration constraints. The problem formulated is non-convex. To obtain the optimal location, we approximate the rate expression to obtain the concave regions and apply alternating optimization. An iterative scheme is proposed to obtain the optimal UAV trajectory, which computes the optimal location in each time slot sequentially, followed by a greedy approach to reach the final location. Simulation results provide useful insights into the optimal location and the UAV trajectory problem and show on an average 16.5% improvement over the benchmark schemes.</p>



40.	<p><a href="#">Transient study of a solar pond under heat extraction from non-convective and lower convective zones considering finite effectiveness of exchangers</a>  S Verma, R Das - Solar Energy, 2021</p> <p><b>Abstract:</b> The transient performance of a salt gradient solar pond, which experiences heat extraction from both gradient and storage regions has been studied for annual performance via accounting for the overall heat transfer coefficient across heat exchangers. The proposed method after reduced complexities is satisfactorily validated with theory and experiment-based results of pertinent literature. The novelty of the work lies in the fact that, the temperature drop across both non-convective and lower-convective zone exchanger surfaces has been accounted by using a local time and space dependent heat transfer coefficient. Here, it takes into the consideration free convection from the pond to the exchanger surface, and forced convection from the exchanger surface to flowing working fluid. Further, temperature variation of thermo-fluidic parameters of water involving, viscosity, density and thermal conductivity is considered. Detailed numerical investigation reveals that by neglecting this coefficient which is assumed in conventional studies, it can lead to significant errors in the prediction of transient temperature profiles in the pond and the exchangers. Calculations reveal an error of about +69% in the annual extraction efficiency and about -9% in entropy production if the conventional assumption is used as opposed to realistic technique presented herein. Interestingly, the present study reveals that there is an optimum radius of exchanger pipe in each of non-convective and lower convective zones that maximises the annual extraction efficiency. This work presents a useful analysis to assess multi zone extraction from solar ponds under transient state in a more practical and accurate manner.</p>
41.	<p><a href="#">Transition-Metal-Free HFIP-Mediated Organo Chalcogenylation of Arenes/Indoles with Thio-/Selenocyanates</a>  P Kalaramna, A Goswami - The Journal of Organic Chemistry, 2021</p> <p><b>Abstract:</b> We have developed a protocol for the synthesis of diaryl thio-/selenoethers by the reaction of aryl chalcogenocyanates with electron rich arenes/hetero arenes via HFIP promoted C–H activation. The reaction produces chalcogenides in good to excellent yields under mild conditions without the need of a transition metal as a catalyst. The HFIP-mediated reactions tolerated a wide range of functional groups and set the stage for the synthesis of diversely decorated chalcogenides. A mechanism involving activation of the C–H bond through hydrogen bonding is proposed.</p> <div data-bbox="646 1396 1185 1585" data-label="Chemical-Block"> <p style="text-align: center;"> <math display="block">\text{R}^1\text{-C}_6\text{H}_4\text{-XCN} + \text{Ar}^2\text{H} \xrightarrow[\text{rt-60 } ^\circ\text{C}]{(1:1) \text{ HFIP/DCE}} \text{R}^1\text{-C}_6\text{H}_4\text{-X-Ar}^2</math> </p> <p style="text-align: center;"> X = S, Se    Ar<sup>2</sup> = arenes, indoles    35 examples  71-95% </p> <ul style="list-style-type: none"> <li>• Transition-metal-free</li> <li>• Mild conditions</li> <li>• Good to excellent yields</li> </ul> </div>
42.	<p><a href="#">Trends in Small Organic Fluorescent Scaffolds for Detection of Oxidoreductase</a>  JS Sidhu, N Kaur, N Singh - Biosensors and Bioelectronics, 2021</p> <p><b>Abstract:</b> Oxidoreductases are diverse class of enzymes engaged in modulating the redox homeostasis and cellular signaling cascades. Abnormal expression of oxidoreductases including thioredoxin reductase, azoreductase, cytochrome oxidoreductase, tyrosinase and monoamine oxidase leads to the initiation of numerous disorders. Thus, enzymes are the promising</p>

	<p>biomarkers of the diseased cells and their accurate detection has utmost significance for clinical diagnosis. The detection method must be extremely selective, sensitive easy to use, long self-life, mass manufacturable and disposable. Fluorescence assay approach has been developed potential substitute to conventional techniques used in enzyme's quantification. The fluorescent probes possess excellent stability, high spatiotemporal ratio and reproducibility represent applications in real sample analysis. Therefore, the enzymatic transformations have been monitored by small activatable organic fluorescent probes. These probes are generally integrated with enzyme's substrate/inhibitors to improve their binding affinity toward the enzyme's catalytic site. As the recognition unit bio catalyzed, the signaling unit produces the readout signals and provides novel insights to understand the biochemical reactions for diagnosis and development of point of care devices. Several structural modifications are required in fluorogenic scaffolds to tune the selectivity for a particular enzyme. Hence, the fluorescent probes with their structural features and enzymatic reaction mechanism of oxidoreductase are the key points discussed in this review. The basic strategies to detect each enzyme are discussed. The selectivity, sensitivity and real-time applications are critically compared. The kinetic parameters and futuristic opportunities are present, which would be enormous benefits for chemists and biologists to understand the facts to design and develop unique fluorophore molecules for clinical applications.</p> <p><b>Graphical Abstract:</b></p> 
43.	<p><a href="#">Vapour transport grown photosensitive GeO<sub>2</sub> thin film</a>  A Choudhury, A Dalal, SMMD Dwivedi, A Ghosh... - Materials Research Bulletin, 2021</p> <p><b>Abstract:</b> GeO<sub>2</sub> thin film (TF) was fabricated by vapour deposition technique in a two zone horizontal quartz tube. Field emission-scanning electron microscopy showed the formation of 200 nm TF on the Si (100) substrate. The X-ray diffraction depicted the presence of the polycrystalline GeO<sub>2</sub> TF. The UV–vis absorption spectrum showed humps at 3.1 eV, 4.0 eV and 5.4 eV. The band anticrossing (BAC) model is modified using the Urbach equation to understand the different transitions in the optical absorption spectrum. We have theoretically calculated the relative refractive index (r.i.) ( of the GeO<sub>2</sub> as 1.8. The temperature dependent current (I)–voltage (V) characteristics and photocurrent of the Au/GeO<sub>2</sub>/p-Si Schottky device predicted the tunnelling of the carriers, presence of oxygen defects at the junction. The device’s temporal response indicated good photosensitivity at all temperatures and a significant increase in photocurrent was obtained as the temperature increased from 303 K to 403 K.</p>

## Graphical Abstract:



**Disclaimer:** This publication digest may not contain all the papers published. Library has compiled the publication data as per the alerts received from Scopus and Google Scholar for the affiliation “Indian Institute of Technology Ropar” for the month of June 2021. The author(s) are requested to share their missing paper(s) details if any, for the inclusion in the next publication digest.